Progress In Electromagnetics Research M, Vol. 18, 89–101, 2011

SKIN EFFECT IN INHOMOGENEOUS EULER-CAUCHY TUBULAR CONDUCTORS

J. A. Brandão Faria

Instituto de Telecomunicações, Instituto Superior Técnico
Technical University of Lisbon
Av. Rovisco Pais, Lisbon, 1049-001 Lisboa, Portugal

Abstract—This paper presents a novel contribution to the analysis of skin effect phenomena in inhomogeneous tubular conductors. For homogeneous tubular geometries the skin effect diffusion equation has an analytical solution described by a combination of Bessel functions, but, when the conductivity and magnetic permeability of the tubular conductor arbitrarily depend on the radial coordinate an analytical solution cannot be found. However, this work shows that simple closed form solutions for the electromagnetic field and conductor internal impedance do exist, provided that a specific type of radial variation of medium parameters is properly chosen — these novel structures are coined here Euler-Cauchy Structures. Analytic and computation results concerning general and particular Euler-Cauchy Structures are presented, validated, and discussed. Future research on this seminal topic may lead to new engineering applications.

1. INTRODUCTION

The skin effect phenomenon is of major concern for high frequency regimes. The topic is usually connected with transmission-line problems, where both the real and imaginary parts of the per unit length (pul) internal impedance of line conductors depend on the frequency, leading to signal attenuation and distortion.

Skin effect analysis has been a research issue for a long time: from circular cylindrical conductors to conductors with more complicated cross sections [1–9]. Recently, the interest in circular and tubular geometries has apparently rebirth [10–21], however, most of published

Received 9 March 2011, Accepted 28 April 2011, Scheduled 2 May 2011
Corresponding author: Prof. J. A. Brandão Faria (brandao.faria@ieee.org).

work has been focused on the development of approximate formulas for internal impedance evaluation of homogeneous structures. Those formulas are basically used to circumvent the troublesome computation of Bessel functions.

Results concerning skin effect analysis of inhomogeneous tubular conductors are very scarce. Nonetheless, the current state of the art in material technology may already allow the radial profile of both the conductivity $\sigma(r)$ and magnetic permeability $\mu(r)$ of cylindrical conductors to be tailored to meet any realistic specification.

In general, the wave equation describing the electromagnetic field (EMF) in radially inhomogeneous conducting media does not have an analytical solution. In this paper, the research problem of finding exact closed form solutions for skin effect phenomena in circular cylindrical tubular geometries with inhomogeneous media is addressed. The goal is to devise appropriate functions for $\sigma(r)$ and $\mu(r)$ that may transform the radial wave equation into a simpler differential equation that exhibits closed form analytical solutions.

The differential equation referred to above is the Euler-Cauchy equation [22]. Inhomogeneous cylindrical structures that fit in the framework of this equation will be coined Euler-Cauchy Structures (ECS).

To the best of our knowledge, the research developed in this paper is an absolutely novel contribution to the area of skin effect analysis.

In addition to its intrinsic theoretical importance, the closed form solutions that have been obtained can be of great help as benchmark tools for checking the accuracy and performance of EMF software packages.

2. FIELD EQUATIONS

For time harmonic regimes ($e^{j\omega t}$) and for the case of very good conductors, $\sigma >> \omega\varepsilon$, the displacement current can always be neglected for frequencies up to the optical range [23], therefore, the frequency-domain Maxwell curl equations read as

$$\begin{cases} \nabla \times \bar{\mathbf{H}} = \bar{\mathbf{J}} + j\omega\bar{\mathbf{D}} \approx \bar{\mathbf{J}} = \sigma\bar{\mathbf{E}} \\ \nabla \times \bar{\mathbf{E}} = -j\omega\bar{\mathbf{B}} = -j\omega\mu\bar{\mathbf{H}} \end{cases} \tag{1}$$

where σ, ε, and μ respectively denote the conductivity, permittivity, and magnetic permeability of the material medium; $\omega = 2\pi f$ is the angular frequency.

Overbar quantities in (1) represent complex amplitudes of field vectors. $\mathbf{H}$ is the magnetic field, $\mathbf{B}$ is the magnetic induction field, $\mathbf{E}$ is the electric field, $\mathbf{D}$ is the electric displacement vector, and $\mathbf{J}$ is the conduction current density.

In addition, from $\nabla \cdot \bar{\mathbf{B}} = 0$, it results $\bar{\mathbf{B}} = \nabla \times \bar{\mathbf{A}}$, where $\bar{\mathbf{A}}$ is the complex amplitude of the magnetic vector potential, with $\nabla \cdot \bar{\mathbf{A}} = 0$ (Coulomb gauge).

Combination of the above results yields

$$\begin{cases} \bar{\mathbf{E}} = -j\omega\bar{\mathbf{A}} \\ \bar{\mathbf{H}} = \left(\nabla \times \bar{\mathbf{A}}\right)/\mu \end{cases} \tag{2}$$

For the particular case of a solid homogeneous circular cylindrical conductor (of radius r_2) with axial currents, the governing equation of the magnetic vector potential $\bar{\mathbf{A}} = \bar{A}(r)\,\vec{e}_z$ is determined, from (1) and (2), as

$$\frac{d^2\bar{A}}{dr^2} + \frac{1}{r}\frac{d\bar{A}}{dr} + \bar{k}^2\bar{A} = 0 \tag{3a}$$

where $\bar{k} = \sqrt{-j\omega\mu\sigma}$ is the complex wave number. Equation (3a) is the Bessel equation of zeroth order [23]. Its solution is well-known:

$$\bar{A} = \frac{\mu\bar{I}}{2\pi r_2\bar{k}}\frac{J_0(\bar{k}r)}{J_1(\bar{k}r_2)} \tag{3b}$$

where J_0 and J_1 are Bessel Functions [22], and $\bar{I}$ denotes the complex amplitude of the sinusoidal current flowing in the conductor.

From (2) and (3), the following results for the electric and magnetic field in the conductor are found [23],

$$\begin{cases} \bar{\mathbf{E}} = \frac{\bar{k}\,\bar{I}}{2\pi\sigma r_2}\frac{J_0(\bar{k}r)}{J_1(\bar{k}r_2)}\,\vec{e}_z \\ \bar{\mathbf{H}} = \frac{\bar{I}}{2\pi r_2}\frac{J_1(\bar{k}r)}{J_1(\bar{k}r_2)}\,\vec{e}_\phi \end{cases}, \quad \text{for } 0 < r < r_2 \tag{3c}$$

The pul internal impedance of the homogeneous cylindrical conductor is [23],

$$\bar{Z} = \frac{\bar{E}(r_2)}{\bar{I}} = \frac{\bar{k}}{2\pi\sigma r_2}\frac{J_0(\bar{k}r_2)}{J_1(\bar{k}r_2)} \tag{3d}$$

For a homogeneous tubular conductor, $\bar{Z}$ is also obtained from (3a), yielding a combination of Bessel functions — see for example [19, 21].

For the general case of inhomogeneous media, where both μ and σ vary with r, the governing equation of the magnetic vector potential is no longer described by (3a).

The new equation for $\bar{A}$ is obtained from (1) and (2), and reads as

$$r^2\frac{d^2\bar{A}}{dr^2} + r\frac{d\bar{A}}{dr}\left(1 - \frac{r}{\mu}\frac{d\mu}{dr}\right) + \left(r\,\bar{k}(r)\right)^2\bar{A} = 0 \tag{4}$$

where $\bar{k}(r)$ is the complex wave number

$$\bar{k}(r) = \sqrt{-j\omega\mu(r)\sigma(r)} \tag{5}$$

In general, for arbitrary $\mu(r)$ and $\sigma(r)$ functions, the solution of (4) can only be found numerically.

As a parenthetical remark it should be added that, in the case of an isolated single conductor, the electric field in (2) is to be interpreted as a purely electric induction field, since its gradient component is absent (the conductor is not charged).

3. EULER-CAUCHY STRUCTURES

Consider a tubular conductor characterized by inner radius r_1 and outer radius r_2 (Fig. 1).

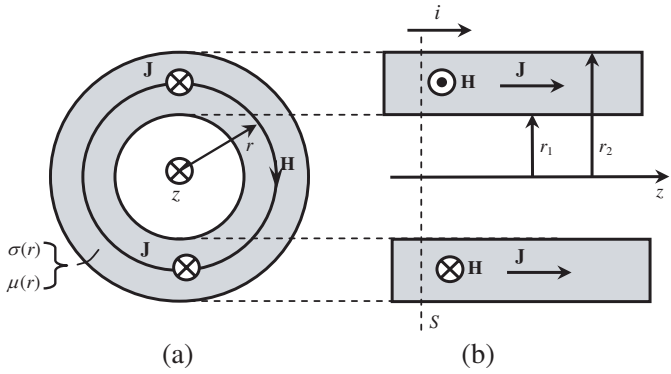

Figure 1. Tubular conductor. (a) Transverse section. (b) Longitudinal section.

For the outer boundary, $r = r_2$, the conductivity is σ_2, the magnetic permeability is μ_2, and the complex wave number $\bar{k}_2$ and the skin depth δ_2 [23], are

$$\bar{k}_2 = \sqrt{-j\omega\mu_2\sigma_2} = \frac{1-j}{\delta_2}; \quad \delta_2 = \sqrt{\frac{2}{\omega\mu_2\sigma_2}} \tag{6}$$

The key idea is to transform the coefficients (set in parentheses) of the second and third terms of the left hand side of (4) into constant coefficients independent of r, so that one may arrive to the following equation

$$r^2\frac{d^2\bar{A}}{dr^2} + \alpha r\frac{d\bar{A}}{dr} + \beta\bar{A} = 0 \tag{7}$$

where

$$\begin{cases} \alpha = 1 - \frac{r}{\mu(r)}\frac{d\mu(r)}{dr} = \text{constant independent of } r \\ \beta = -j\omega r^2 \mu(r)\sigma(r) = \left(\bar{k}_2 r_2\right)^2 = \text{constant independent of } r \end{cases} \tag{8}$$

The result in (7) describes the so-called homogeneous second order Euler-Cauchy equi-dimensional equation [22]. Henceforth, any cylindrical structure whose material medium is described by constitutive parameters $\mu(r)$ and $\sigma(r)$ conforming to (8) will be called an ECS.

The solution of (7) can be written in closed form [22], for $r_1 \leq r \leq r_2$, as

$$\bar{A}(r) = Fr^{m_1} + Gr^{m_2} \tag{9}$$

where m_1 and m_2 are the roots of the characteristic equation

$$m^2 + (\alpha - 1)m + \beta = 0; \quad \begin{cases} m_1 + m_2 = 1 - \alpha \\ m_1 m_2 = \beta \end{cases} \tag{10}$$

The constants F and G in (9) will be determined by using the pertinent boundary conditions of the problem; see (15)–(16).

In (8), the top equation for α, leads to

$$\mu(r) = \mu_2 \left(\frac{r}{r_2}\right)^p; \quad p = 1 - \alpha \tag{11}$$

where p is a real number, and $r_1 \leq r \leq r_2$.

Combining (11) with the bottom equation for β, in (8), leads to

$$\sigma(r) = \sigma_2 \left(\frac{r_2}{r}\right)^{2+p} \tag{12}$$

From (11) and (12), the complex roots of the characteristic equation in (10) are found to satisfy

$$\begin{cases} m_{1,2} = \frac{p}{2} \pm \sqrt{\left(\frac{p}{2}\right)^2 - \left(\bar{k}_2 r_2\right)^2} \\ m_1 m_2 = \beta = \left(\bar{k}_2 r_2\right)^2 \in \Im^{(-)} \\ m_1 + m_2 = p \in \Re \\ \text{Im}\{m_1\} = -\text{Im}\{m_2\} \\ \text{Re}\{m_1\}\,\text{Re}\{m_2\} < 0 \end{cases} \tag{13}$$

The set of conditions in (13) points out that, independently of p, one root is on the 1st quadrant of the complex plane, whereas the other is on the 3rd. Hereafter, without loss of generality, m_1 is considered to belong to the 1st quadrant.

For the sake of conciseness, the brief notation **ECS-C$_\mathbf{p}$** is introduced to classify different types of Euler-Cauchy structures, where underscript p is a reminder for the power law variation assigned to $\mu(r)$.

4. GENERAL SOLUTION OF THE WAVE EQUATION FOR ECS-Cp

From (2) and (9), the complex amplitude of the azimuthal magnetic field can be determined through

$$\bar{H}(r) = -\frac{1}{\mu(r)}\frac{d\bar{A}}{dr} = -\frac{1}{\mu(r)}\left(Fm_1 r^{m_1-1} + Gm_2 r^{m_2-1}\right) \tag{14}$$

The F and G complex constants are evaluated in (16) by taking into account the boundary conditions

$$\bar{H}(r_1) = 0\ ;\ \ \bar{H}(r_2) = \bar{I}/(2\pi r_2) \tag{15}$$

The boundary conditions in (15) are a direct consequence of the application of Ampère Law to circumferential paths of radius r_1 and r_2, respectively [23],

$$F = \frac{\mu_2 \bar{I}}{2\pi m_1}\frac{r_1^{m_2}}{r_1^{m_1}r_2^{m_2} - r_1^{m_2}r_2^{m_1}}\ ;\quad G = -F\frac{m_1}{m_2}\,\frac{r_1^{m_1}}{r_1^{m_2}} \tag{16}$$

Substituting (16) into (14), yields

$$\bar{H}(r) = \frac{\bar{I}}{2\pi r}\frac{(r_1/r)^{m_1} - (r_1/r)^{m_2}}{(r_1/r_2)^{m_1} - (r_1/r_2)^{m_2}} \tag{17}$$

The complex amplitude of the axial current density in the conductor, $\bar{J}(r) = -j\omega\sigma(r)\bar{A}(r)$, is obtained from (2), (9), (12) and (16)

$$\bar{J}(r) = \frac{\bar{I}}{2\pi r^2}\frac{m_2(r_1/r)^{m_2} - m_1(r_1/r)^{m_1}}{(r_1/r_2)^{m_1} - (r_1/r_2)^{m_2}} \tag{18}$$

At last, the frequency-dependent pul internal impedance $\bar{Z}$ of the tubular conductor is determined as

$$\bar{Z} = R + jX = \frac{\bar{E}(r_2)}{\bar{I}} = \frac{\bar{J}(r_2)}{\sigma_2 \bar{I}} = \frac{m_2(r_1/r_2)^{m_2} - m_1(r_1/r_2)^{m_1}}{2\pi\sigma_2 r_2^2\left((r_1/r_2)^{m_1} - (r_1/r_2)^{m_2}\right)} \tag{19}$$

For the limit case of a solid inhomogeneous cylindrical conductor ($r_1 \to 0$), the pul internal impedance in (19) transforms into $\bar{Z} = j\omega\mu_2/(2\pi m_1)$. This result was obtained from (19) by taking into consideration that $\mathrm{Re}(m_1) > 0$ and $\mathrm{Re}(m_2) < 0$.

5. PARTICULAR SOLUTIONS OF THE WAVE EQUATION FOR ECS-Cp

Next, for illustration purposes, the general results derived in Section 4 are particularized for ECS of class p, with $p = 0$ and $p = -2$.

The analysis of these two particular cases is motivated by the special circumstance that $p = 0$ corresponds to the situation of invariant permeability (magnetic homogeneity conditions), while $p = -2$ corresponds to invariant conductivity (electric homogeneity conditions).

5.1. ECS-C_0

Here, the tubular conductor is characterized by $\mu = \mu_2$, whereas the conductivity varies with $1/r^2$. The roots of the characteristic equation in (13) are $m_1 = -m_2 = m = (1 + j)(r_2/\delta_2)$.

From (17), (18), and (19) we find

$$\bar{H}(r) = \frac{\bar{I}}{2\pi r}\left(\frac{r}{r_2}\right)^m \left(\frac{1-(r_1/r)^{2m}}{1-(r_1/r_2)^{2m}}\right) \tag{20}$$

$$\bar{J}(r) = \frac{m\bar{I}}{2\pi r^2}\left(\frac{r}{r_2}\right)^m \left(\frac{1+(r_1/r)^{2m}}{1-(r_1/r_2)^{2m}}\right) \tag{21}$$

$$\bar{Z} = R + jX = R_{HF}(1+j)\left(\frac{1+(r_1/r_2)^{2m}}{1-(r_1/r_2)^{2m}}\right) \tag{22}$$

where $R_{HF} = 1/(2\pi r_2 \delta_2 \sigma_2)$ is the high-frequency limit of the pul resistance of a homogeneous cylinder (μ_2, σ_2) of radius r_2.

For the solid cylinder case $r_1 \to 0$, we obtain from (22): $\bar{Z} = R_{HF}(1 + j)$. Remarkably, the real and imaginary parts of the pul impedance turn out to be equal to each other no matter the frequency. This surprising conclusion contrasts with the well-known result for homogeneous cylindrical conductors, where $R(\omega) > X(\omega)$ [23]. Another interesting fact is that, for the inhomogeneous cylinder, both R and X depend on the square root of the frequency from DC to high-frequency — bear in mind that this type of behavior in homogeneous cylinders is exceptionally observed for strong skin effect phenomena ($\omega \to \infty$) [23].

5.2. ECS-C_{-2}

Here, the tubular conductor is characterized by $\sigma = \sigma_2$, whereas the permeability varies with $1/r^2$. The roots of the characteristic equation in (13) are $m_1 = m$ and $m_2 = -(2 + m)$, where $m + 1 = n = \sqrt{1 + 2j(r_2/\delta_2)^2}$.

From (17), (18), and (19) we find

$$\bar{H}(r) = \frac{\bar{I}}{2\pi r_2}\left(\frac{r}{r_2}\right)^n \left(\frac{1-(r_1/r)^{2n}}{1-(r_1/r_2)^{2n}}\right) \tag{23}$$

$$\bar{J}(r) = \frac{\bar{I}}{2\pi r_2^2}\left(\frac{r}{r_2}\right)^{n-1} \left(\frac{(n+1)+(n-1)\,(r_1/r)^{2n}}{1-(r_1/r_2)^{2n}}\right) \tag{24}$$

$$\bar{Z} = R + jX = \frac{1}{2\pi\sigma_2 r_2^2}\left(1 + n\left(\frac{1+(r_1/r_2)^{2n}}{1-(r_1/r_2)^{2n}}\right)\right) \tag{25}$$

6. COMPUTATION RESULTS

For exemplification purposes the following fixed parameters will be used $r_2 = 3r_1 = 3\,\text{mm}$; $\sigma_2 = 0.5\times10^7\,\text{S/m}$; $\mu_2 = \mu_0 = 4\pi\times10^{-7}\,\text{H/m}$, which yield an absolute value for the wave number, (6), $\left|\bar{k}_2\right| = 2\pi\sqrt{f}$ rad/m.

Without loss of generality, the rms value of the sinusoidal current in the tubular conductor is chosen as $I_{\text{rms}} = 1\,\text{A}$.

6.1. ECS-C$_0$

Consider $\mu(r) = \mu_2$, and $\sigma(r) = \sigma_2(r_2/r)^2$, with σ varying in the range $\sigma(r) \in \left[0.5\times10^6, 4.5\times10^7\right]\,\text{S/m}$.

Making use of (20) and (21), graphics of the radial variation of the rms value of the magnetic field and current density were obtained for $f = 0.5\,\text{Hz}$, $f = 50\,\text{kHz}$, and $f = 0.5\,\text{MHz}$. Results are depicted in Fig. 2, showing, for low frequencies, that the current density J has its larger values in the vicinity of r_1 because, there, the conductivity is higher.

The real and imaginary parts of the pul internal impedance, (22), are presented in Fig. 3 as a function of the frequency (up to 0.1 MHz). The superposed circle marks correspond to numerical results obtained by employing a multi-layer technique where the inhomogeneous medium is broken down into 100 concentric homogeneous layers [24], — discrepancies are not visible.

6.2. ECS-C$_{-2}$

Consider $\sigma(r) = \sigma_2$ and $\mu(r) = \mu_2(r_2/r)^2$, with μ varying in the range $\mu(r) \in [\mu_0, 9\mu_0]$.

Making use of (23) and (24), graphics of the radial variation of the rms value of the magnetic field and current density were obtained for

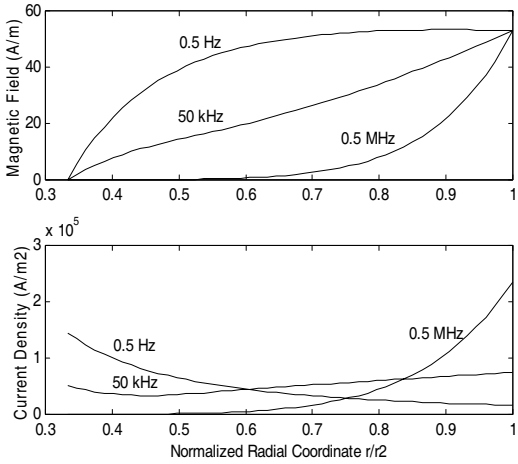

Figure 2. Plots of $H_{rms}(r)$ and $J_{rms}(r)$ against the normalized radial coordinate r/r_2, for three different frequencies, for an ECS of class 0.

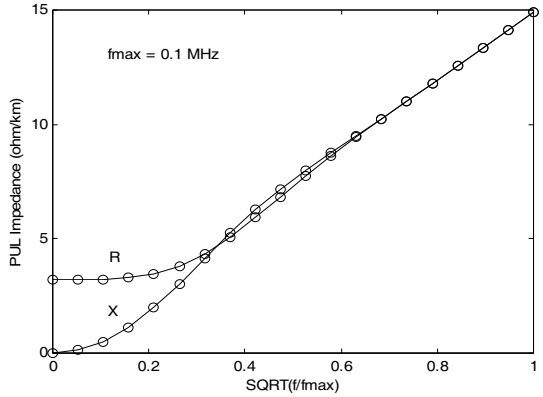

Figure 3. Pul internal impedance against the square root of the frequency, for an ECS of class 0.

$f = 0.5\,\text{Hz}$, $f = 50\,\text{kHz}$, and $f = 0.5\,\text{MHz}$. Results are depicted in Fig. 4, showing, for low frequencies, that the rate of growth of the magnetic field H is smaller than the one observed in Fig. 2 (for a magnetically homogeneous conductor), this is so because the permeability increases for decreasing values of r.

The real and imaginary parts of the pul internal impedance, (25), are presented in Fig. 5 as a function of the frequency (up to 0.1 MHz). The superposed circle marks correspond to numerical results obtained employing a multi-layer technique [24], — discrepancies are not visible.

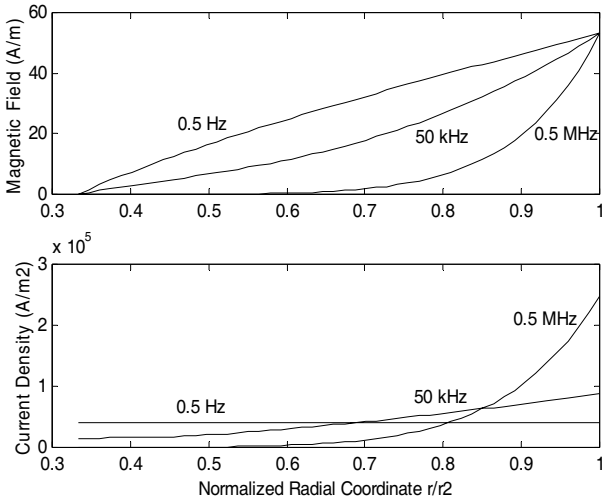

Figure 4. Plots of $H_{rms}(r)$ and $J_{rms}(r)$ against the normalized radial coordinate r/r_2, for three different frequencies, for an ECS of class -2.

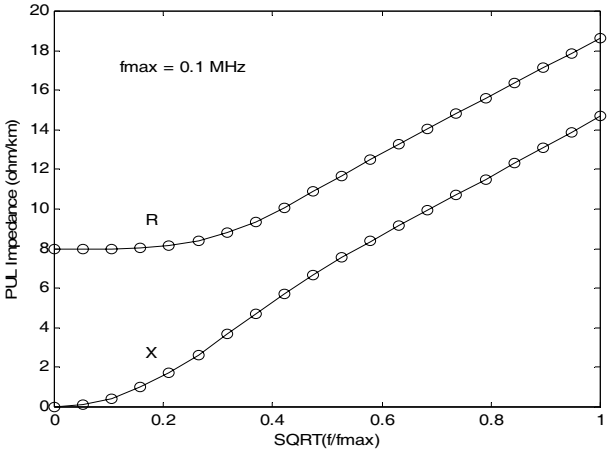

Figure 5. Pul internal impedance against the square root of the frequency, for an ECS of class -2.

7. CONCLUSION

A novel theoretical contribution to the analysis of skin effect phenomena in radially inhomogeneous tubular conductors was presented, whereby, to the best of our knowledge, the concept of Euler-Cauchy Structure was introduced for the first time: $\mu(r) \propto r^p$ and $\sigma(r) \propto r^{-(2+p)}$, where the arbitrary real valued parameter p defines the ECS class.

The specific radial variation assigned to the permeability and conductivity of the tubular conductor was shown to allow for the existence of simple closed form analytical solutions of the diffusion equation — a remarkable feature for inhomogeneous structures, since, ordinarily, such an equation can only be solved by numerical means.

This paper is, by its own nature, a theoretical work. The technical implications and practical significance of Euler-Cauchy structures are not clear yet. However, most technological applications occur after previous theoretical developments have been put forward. Since the inhomogeneity factor p (a real number) can be chosen arbitrarily, the possibilities to explore are immense (future work).

Nowadays, inhomogeneous structures made from multilayered conductors are already produced for the purpose of losses mitigation in superconductors. It is hoped that this work may trigger interest enough to the point of leading to practical engineering applications in that field, or others.

REFERENCES

1. Dwight, H., "Skin effect in tubular and flat conductors," *AIEE Trans.*, Vol. 37, Part. II, 1379–1403, 1918.
2. Cockcroft, J., "Skin effect in rectangular conductors at high frequencies," *Proc. Roy. Soc.*, Vol. 122, 533–542, 1929.
3. Arnold, A., "The alternating current resistance of tubular conductors," *J. IEE*, Vol. 78, 580–593, 1936.
4. Silvester, P., "The accurate calculation of skin effect in conductors of complicated shape," *IEEE Trans. Power App. Syst.*, Vol. 87, No. 3, 735–742, 1968.
5. Tegopoulos, J. and E. Kriezis, "Eddy current distribution in cylindrical shells of infinite length due to axial currents," *IEEE Trans. Power App. Syst.*, Vol. 90, No. 3, 1278–1286, 1971.
6. Waldow, P. and I. Wolff, "The skin-effect at high frequencies," *IEEE Trans. Microw. Theory Tech.*, Vol. 33, No. 10, 1076–1081, 1985.

7. Costache, G., "Finite element method applied to skin-effect problems in strip transmission lines," *IEEE Trans. Microw. Theory Tech.*, Vol. 35, No. 11, 1009–1013, 1987.
8. Tsuk, M. and J. Kong, "A hybrid method for the calculation of the resistance and inductance of transmission lines with arbitrary cross sections," *IEEE Trans. Microw. Theory Tech.*, Vol. 39, No. 8, 1338–1347, 1991.
9. Silveira, F. and J. Lima, "Skin effect from extended irreversible thermodynamics perspective," *Journal of Electromagnetic Waves and Applications*, Vol. 24, No. 2–3, 151–160, 2010.
10. Barmada, S., L. Rienzo, N. Ida, and S. Yuferev, "The use of surface impedance conditions in time domain problems: Numerical and experimental validation," *Appl. Comput. Electromag. Soc. Journal*, Vol. 19, No. 2, 76–83, 2004.
11. Barmada, S., L. Rienzo, N. Ida, and S. Yuferev, "Time domain surface impedance concept for low frequency electromagnetic problems. Part II: Application to transient skin and proximity effect problems in cylindrical conductors," *IEE Proc. Sci. Meas. Technol.*, Vol. 154, No. 5, 207–216, 2005.
12. Rong, A. and A. Cangelaris, "Note on the definition and calculation of the per-unit-length internal impedance of a uniform conducting wire," *IEEE Trans. Electrom. Comp.*, Vol. 49, No. 3, 677–681, 2007.
13. Morsey, J., V. Okhmatovski, and A. Cangelaris, "Finite-thickness conductor models for full-wave analysis of interconnects with a fast integral equation method," *Proc. IEEE 11th Topical Meeting on Electrical Performance of Electronic Packaging*, Monterey, USA, Oct. 2002.
14. Zutter, D., H. Rogier, L. Knockaert, and J. Sercu, "Surface current modelling of the skin effect for on-chip interconnections," *IEEE Trans. Adv. Packaging*, Vol. 30, No. 2, 342–349, 2007.
15. Morgan, V., R. Findlay, and S. Derrah, "New formula to calculate the skin effect in isolated tubular conductors at low frequencies," *IEE Proc. Sci. Meas. Technol.*, Vol. 147, No. 4, 169–171, 2000.
16. Mingli, W. and F. Yu, "Numerical calculations of internal impedance of solid and tubular cylindrical conductors under large parameters," *IEE Proc. Generation Transm. Distribution*, Vol. 151, No. 1, 67–72, 2004.
17. Coufal, O., "Current density in a long solitary tubular conductor," *J. Physics A: Math. Theor.* Vol. 41, No. 14, 145401 (14pp), 2008.

18. Rienzo, L., S. Yuferev, and N. Ida, "Calculation of energy-related quantities of conductors using surface impedance concept," *IEEE Trans. Magnetics*, Vol. 44, No. 6, 1322–1325, 2008.
19. Vujevic, S., V. Boras, and P. Sarajcev, "A novel algorithm for internal impedance computation of solid and tubular cylindrical conductors," *Int. Rev. Electric. Eng.*, Vol. 4, No. 6, 1418–1425, 2009.
20. Knight, D., "Practical continuous functions and formulae for the internal impedance of cylindrical conductors," http//www.g3ynh.info/ zdocs/comps/Zint.pdf, March 2010.
21. Lovric, D., V. Boras, and S. Vujevic, "Accuracy of approximate formulas for internal impedance of tubular cylindrical conductors for large parameters," *Progress In Electromagnetics Research M*, Vol. 16, 171–184, 2011.
22. Wylie, C., *Advanced Engineering Mathematics*, McGraw-Hill, New York, 1975.
23. Faria, J., *Electromagnetic Foundations of Electrical Engineering*, Wiley, Chichester, UK, 2008.
24. Faria, J., "A matrix approach for the evaluation of the internal impedance of multilayered cylindrical structures," *Progress In Electromagnetics Research B*, Vol. 28, 351–367, 2011.